

Article

# Harnessing Physics-Informed Neural Networks for Performance Monitoring in SWRO Desalination

Saloua Helali <sup>1</sup>, Shadia Albalawi <sup>1</sup> and Nizar Bel Hadj Ali <sup>2,\*</sup>

<sup>1</sup> Department of Physics, Faculty of Science, University of Tabuk, King Faisal Road, Tabuk 47512, Saudi Arabia; s.helali@ut.edu.sa (S.H.); sh.albalawi@ut.edu.sa (S.A.)

<sup>2</sup> Modeling in Civil Engineering and Environment (MCEE), National School of Engineers, University of Gabes, Street Omar Elkhattab, Zrig, Gabes 6029, Tunisia

\* Correspondence: nizar.belhadjali@enig.rnu.tn

**Abstract:** Seawater Reverse Osmosis (SWRO) desalination is a critical technology for addressing global water scarcity, yet its performance can be hindered by complex process dynamics and operational inefficiencies. This study investigates the revolutionary potential of Physics-Informed Neural Networks (PINNs) for modeling SWRO desalination processes. PINNs are subsets of machine learning algorithms that incorporate physical information to help provide physically meaningful neural network models. The proposed approach is here demonstrated using operating data collected over several months in a Seawater RO plant. PINN-based models are presented to estimate the effects of operating conditions on the permeate TDS and pressure drop. The focus is on the feed water temperature variations and progressive membrane deterioration caused by fouling. Predictive models generated using PINNs showed high performances with a determination coefficient of 0.96 for the permeate TDS model and 0.97 for the pressure drop model. Results show that the use of PINNs significantly enhances the ability to predict membrane fouling and produced water quality, thereby supporting informed decision-making for RO process control.

**Keywords:** physics-informed neural networks; reverse osmosis; SWRO desalination; performance monitoring



Academic Editors: Mavromatis Theodoros, Thomas Alexandridis and Vassilis Aschonitis

Received: 25 December 2024

Revised: 17 January 2025

Accepted: 18 January 2025

Published: 22 January 2025

**Citation:** Helali, S.; Albalawi, S.; Bel Hadj Ali, N. Harnessing Physics-Informed Neural Networks for Performance Monitoring in SWRO Desalination. *Water* **2025**, *17*, 297. <https://doi.org/10.3390/w17030297>

**Copyright:** © 2025 by the authors. Licensee MDPI, Basel, Switzerland. This article is an open access article distributed under the terms and conditions of the Creative Commons Attribution (CC BY) license (<https://creativecommons.org/licenses/by/4.0/>).

## 1. Introduction

Global demand for freshwater has undergone a sustained increase as a result of economic development and increasing population. The UN World Water Development Report (2023) estimated that a quarter of the world's population lacks access to clean drinking water [1]. In response to this situation, many countries around the world are increasingly investing in advanced technologies and infrastructure to secure a sustainable and reliable supply of freshwater [2]. In this context, technologies for desalination have become a practical way to deal with the shortage of clean drinking water [3]. The desalination process, involving the separation of dissolved solids from seawater or brackish water, has become the primary source of fresh water for both municipal and industrial sectors in some parts of the world, particularly North Africa and the Middle East [2].

Reverse Osmosis (RO) is currently the most popular desalination technology due to a lower specific consumption of energy and its reliability compared with other available technologies [4]. About 70% of desalination procedures used globally are currently membrane-based. However, monitoring the performance of a full-scale RO process is challenging. This task requires accurately representing the membrane permeability, selectivity, and fouling behavior. Accurate modeling of the RO process is crucial for inferring

the basic features that serve for process diagnostic and prognostic tasks [5]. There are, in contrast, major obstacles to developing accurate and comprehensive deterministic models describing RO process behavior. Major obstacles include (1) variability in feed composition and temperature, (2) difficulties in capturing time-dependent factors like fouling, aging, and chemical cleaning, and (3) difficulties in incorporating accurate representations of fouling and scaling mechanisms since they are not fully understood [3,6].

As mentioned earlier, the effectiveness of RO desalination plants depends on various factors, including the chosen technology, operating parameters, and the characteristics of the feed water. Experimental studies are expensive and time-consuming. Therefore, developing models to predict and evaluate desalination system performance is highly valuable. Data-driven approaches, renowned for their ability to model intricate systems, offer promising solutions for forecasting the performance of desalination units. Recently, there has been a growing interest in using machine learning (ML) tools to handle intricate modeling tasks related to RO processes [7]. This was motivated by data availability and recent advances in computing capabilities. Recent research works showed that ML can be utilized to optimize the performance of RO plants by real-time monitoring performance, predicting maintenance requirements, optimizing energy consumption, and providing early warning about deviations from normal functioning [7–11]. Consequently, ML can help ensure the overall efficiency and sustainability of RO plants [12]. In this context, Mohammed et al. [13] evaluated ensemble and non-ensemble ML models for estimating the performance of RO membranes. The salt rejection was predicted using 13 input parameters, such as time-dependent, water characteristics, and operational parameters. Mahadeva et al. [14,15] proposed a modified Whale Optimization Algorithm (MWOA) hybridized with Artificial Neural Networks (ANNs) to evaluate the permeate flux in a RO desalination plant. Essa et al. [16] created a hybrid machine learning model to predict permeate flow and energy savings of an RO unit using an Artificial Hummingbird Algorithm (AHA)-estimated Long Short-term Memory (LSTM) neural network. Karimanzira and Rauschenbach [16] employed Multivariate Temporal Convolutional Neural networks (MTCNs) to predict membrane fouling utilizing measurable multiple indicators including RO operation data, membrane characteristics, feed water quality, and Cleaning In Place (CIP). Alhuyi Nazari et al. [17] presented a comprehensive review of the applications of different data-driven approaches in the performance modeling of solar-based desalination units.

In most cases, these previous studies used conventional ML algorithms to train predictive models for the RO process based only on collected data at specific RO plants. Though largely employed in many engineering fields, purely data-driven models may suffer from a lack of generality [18]. In many cases, ML-based models may be exploitable only within the narrow domains from which the training data were sourced, which may not adequately capture the complexity of real-world systems. To accommodate the modeling of complex systems effectively, a balanced strategy that incorporates both data-driven and physics-based models is essential [19]. To fill in this scientific gap, a novel ML methodology called Physics-Informed Neural Networks was proposed by Raissi et al. [20]. Neural networks known as PINNs use model equations as part of their internal structure. It is assumed that informing the network of physical principles can amplify the information content of the data used by the learning algorithm, allowing it to achieve more accurate predictions even when only a few training examples are available [19,21,22].

Although PINNs have been used for a wide range of applications, their application in RO desalination process modeling remains underexplored. To address these issues, this paper explores the use of PINNs for the estimation of the RO procedure, which represents the main novelty of the proposed study. The proposed methodology integrates data and mathematical models and implements them through neural networks. More specifically,

the solution–diffusion model equations describing the RO process behavior are embedded directly into the neural network’s loss function. This ensures that the neural network predictions not only fit the input training data but also obey the mathematical equations governing the RO process. The proposed PINN framework is showcased using operation data collected at a seawater RO desalination plant. The studied RO plant was instrumented to monitor the quality, flow, pressure, and temperature of feed water, permeate, and concentrate. The hybrid approach integrating the solution–diffusion equations is used to train a predictive model for the studied RO process. The study results reveal that the use of PINNs offers promising solutions for forecasting the performance of RO desalination units paving the way for an optimized management of such plants.

The remainder of this paper begins with a description of the RO desalination model based on the solution–diffusion equations. This section is followed by a general description of the PINN approach and how it integrates the RO model equations. A case study is presented in Section 4. The collected data and the trained PINN model are presented. Section 4 presents and analyzes the case study’s findings, which are followed by some concluding thoughts in Section 5.

## 2. RO Desalination Model

The mathematical modeling of the seawater RO desalination process is mainly based on solution–diffusion transport equations [23]. Amongst all other modeling alternatives, solution–diffusion equations are widely employed to model the transport of solvent and solute across an RO membrane. In the subsequent paragraphs, we briefly summarize the model’s basic equations and refer the reader to [24–28] for a more detailed presentation of the model.

The diffusion of water across a semi-permeable RO membrane can be represented by the following equation, which is based on the solution–diffusion model.

$$J_w = A_w(\Delta P - \Delta\pi) \quad (1)$$

In Equation (1),  $J_w$  is the permeate flux,  $A_w$  is the membrane permeability coefficient at operating temperature,  $\Delta P$  is the pressure difference between the two sides of the membrane, and  $\Delta\pi$  is the osmotic pressure difference across the surface of the membrane.

The permeate flow rate  $Q_p$  is obtained by adding up the flow contributions from all membrane elements taking into consideration the total membrane area  $S_m$  (Equation (2))

$$Q_p = S_m J_w \quad (2)$$

The solute transport equation is formulated as follows:

$$J_s = B_s(C_f - C_p) = C_p J_w \quad (3)$$

where  $J_s$  is the solute flux through the membrane and  $B_s$  is the solute permeability coefficient of the membrane.  $C_f$  is the solute concentration in the feed stream and  $C_p$  is the solute concentration in the permeate stream.

The water permeability constant  $A_w$  (Equation (1)) is one of the main factors influencing the performance of the RO process. It depends on temperature, and it is also affected by membrane fouling. At a specified temperature, this coefficient can be determined by

applying a temperature correction factor to the permeate intrinsic permeability constant,  $A_{25}$ , as specified by Equation (4) [24].

$$\begin{aligned} A_w &= A_{25} \times e^{[0.0343(T-25)]} \text{ for } T < 25 \text{ }^\circ\text{C} \\ A_w &= A_{25} \times e^{[0.0307(T-25)]} \text{ for } T > 25 \text{ }^\circ\text{C} \end{aligned} \quad (4)$$

Fouling negatively impacts membrane performance as the deposition and accumulation of foulants on the membrane surface leads to a reduction in the permeate flux and significantly alters permeability [29]. Ruiz Garca and Nuez [28] investigated the progressive deterioration of membrane permeability caused by fouling. They proposed a correction flow factor applied to water permeability constant  $A_w$ . The approach proposed in [28] is adopted in this study. The solute permeability coefficient  $B_s$  is also dependent on the temperature of the feedwater. A correction factor should be utilized to the intrinsic solute permeability coefficient  $B_{25}$  to yield the value corresponding to the desired specified temperature (Equation (5)).

$$\begin{aligned} B_s &= B_{25} \times e^{[1+0.05(T-25)]} \text{ for } T < 25 \text{ }^\circ\text{C} \\ B_s &= B_{25} \times e^{[1+0.08(T-25)]} \text{ for } T > 25 \text{ }^\circ\text{C} \end{aligned} \quad (5)$$

The change in the osmotic pressure  $\Delta\pi$  in Equation (1) is calculated as formulated in Equation (6).

$$\Delta\pi = \pi_m - \pi_p \quad (6)$$

where  $\pi_m$  is the osmotic pressure at the surface of the active layer of the membrane and  $\pi_p$  is the RO permeate osmotic pressure [26].

The net applied hydraulic pressure  $\Delta P$  in Equation (1) is given by Equation (7).

$$\Delta P = P_f - \left( \frac{\Delta P_{fb}}{2} \right) \quad (7)$$

where  $P_f$  is the feedwater pressure in the RO system and  $\Delta P_{fb}$  is the pressure drop at the feed side of membrane elements [30].

The percentage of feedwater that is converted into clean, usable water (permeate) is the recovery rate  $R$  expressed in Equation (8). Recovery is a crucial factor that significantly impacts the efficiency and cost-effectiveness of the desalination process.

$$R = \frac{Q_p}{Q_f} \quad (8)$$

In Equation (8),  $Q_f$  is the RO feedwater flow rate.

### 3. Physics-Informed Neural Networks

The aim of a neural network is to obtain an estimate of the mapping from the input  $x$  to the output  $y$ :

$$\bar{y} = \mathcal{N}(x; \theta) \quad (9)$$

In Equation (9),  $\mathcal{N}(x; \theta)$  is a neural network with weights  $\theta$ . Through a training phase, the network weights are determined by solving an optimization problem that minimizes a loss function  $\mathcal{L}_0$ . The goal of the loss function is to match the neural network output with the training input data.

$$\mathcal{L}_0(x; \theta) = \langle y^* - \mathcal{N}(x; \theta) \rangle \quad (10)$$

If the physics of the system can be estimated, the loss function can be augmented to embed a physics-informed term  $\mathcal{L}_{phys}$  (Equation (2)).

$$\mathcal{L}_{phys}(x; \theta) = \langle y^* - \mathcal{F}(x; y; \theta_s) \rangle \quad (11)$$

In Equation (11), the function  $\mathcal{F}(x; y; \theta_s)$  describes the physics of the system through a mathematical model, allowing the determination of an estimate of the response based on the input data. For the present study, the function  $\mathcal{F}$  is built based on the solution–diffusion model equations describing the reverse osmosis process (Equations (1)–(8)). Figure 1 shows the schematic diagram of the PINN approach including a data fitness loss function ( $\mathcal{L}_0$ ) and a physics-informed loss function ( $\mathcal{L}_{phys}$ ).

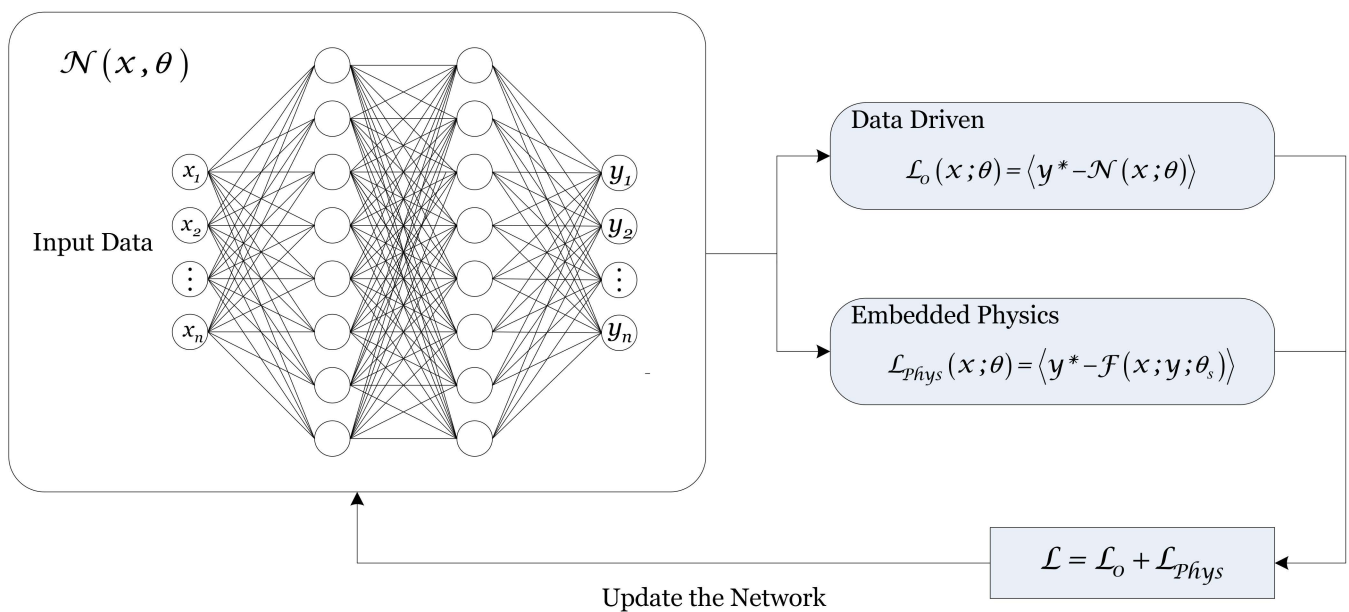


**Figure 1.** Schematic diagram of the PINN. The diagram shows a physics-informed loss function embedded into a typical data-driven neural network scheme.

#### 4. Case Study

The PINN framework described in Section 3 is showcased in this section using operation data collected at a seawater desalination plant using RO technology. The studied RO plant was instrumented to monitor the quality, flow, pressure, and temperature of feed water, permeate, and concentrate. Collected data is here used to train a predictive ML model using PINN. The following paragraphs present the studied SWRO plant, the collected data, and the trained PINN model.

##### 4.1. Description of the Studied SWRO Plant

The studied SWRO desalination plant is schematically illustrated in Figure 2. The feed water is driven by a high-pressure pump through the RO train designed as a two-pass configuration. The first pass has a unique stage with 285 Presser Vessels (PVs) operated in parallel. The second pass is organized in two stages. The first stage has 66 PVs while the second stage has only 27 parallel PVs. In each PV, a series of seven spiral wound elements is installed. The RO elements are composed of Dow FILMTEC® membranes, Minneapolis, MN, USA (Model: SW30HR-440). The concentrate from the second pass is mixed with seawater and again driven to the first pass. In the second pass, the concentrate of the first PV stage is fed to the second stage with no additional pressure. The permeate from both PV stages of the second pass is collected and piped for further processing. The concentrate

is driven to an evaporation pond. The RO plant operates at 42% recovery under a constant flow rate. The feed water had a Total Dissolved Solids (TDS) level of over 42g/L and was mainly composed of Sodium (Na), Chlorine (Cl), and Sulfate (SO<sub>4</sub>). Small quantities of other components are also present, including Magnesium (Mg), Calcium (Ca), Potassium (K), and Fluorine (F). The RO target is to produce freshwater with a TDS not exceeding 100 mg/L. To sustain such a performance level, the water quality parameters and RO plant operation data were continuously monitored. Some of the monitoring data were made available by the plant owners. This dataset is the starting point of the work presented in the subsequent paragraphs.

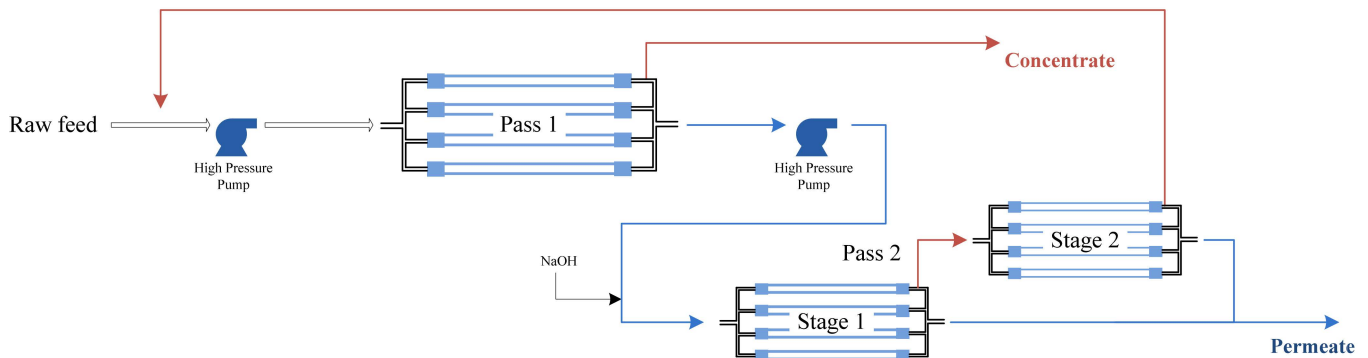


**Figure 2.** Schematic of the studied SWRO plant. The process comprises two-pass RO units. The first pass includes a unique stage whereas the second pass is organized in two stages.

#### 4.2. Collected Data

The monitoring dataset includes measurements undertaken for 760 operating days during which two membrane cleaning (MC) operations were performed. The first MC was performed at 260 days and the second at 580 days. The feed water was sampled and analyzed to explore major ion composition and characteristics. TDS was converted from electrical conductivity. In addition to TDS, the data comprise the flow rate, pressure, and temperature of the feed water, whereas output operation parameters are the permeate TDS, flow rate, and pressure (including interstage pressure). Some statistical details about the gathered dataset variables are displayed in Table 1.

**Table 1.** Statistics of the dataset variables.

Variable	Min	Max	Median	Mean	Std Dev
Temperature (°C)	12.6	29.4	21.1	21.1	5.1
Feed TDS (mg/L)	41,270.5	44,085.1	42,565.0	42,526.8	544.1
Feed Flow (m <sup>3</sup> /day)	68,135.8	75,447.6	72,496.7	72,356.4	1643.4
Feed Pressure (10 <sup>5</sup> Pa)	68.0	74.18	71.45	71.33	1.04
Permeate TDS (mg/L)	57.13	105.57	77.46	76.67	10.47
Pressure drop (10 <sup>5</sup> Pa)	6.3	10.2	7.9	7.9	1.0

The variations in the feed water temperature during the monitoring period are displayed in Figure 3. Feed water temperature changed drastically following seasonal variations. Temperatures ranged between 12 °C and 22 °C during the cold season (November to February). However, plant records showed that the temperature ranged between 24 °C to 30 °C during the hot season (May to October). Inevitably, temperature variations affect permeate quality since permeate TDS is significantly dependent on feed water temperature. Under constant operating flow and pressure, high temperatures increase salt passage through RO membranes, leading to higher TDS. This makes feed temperature one of the major operating parameters to closely monitor in an RO plant.

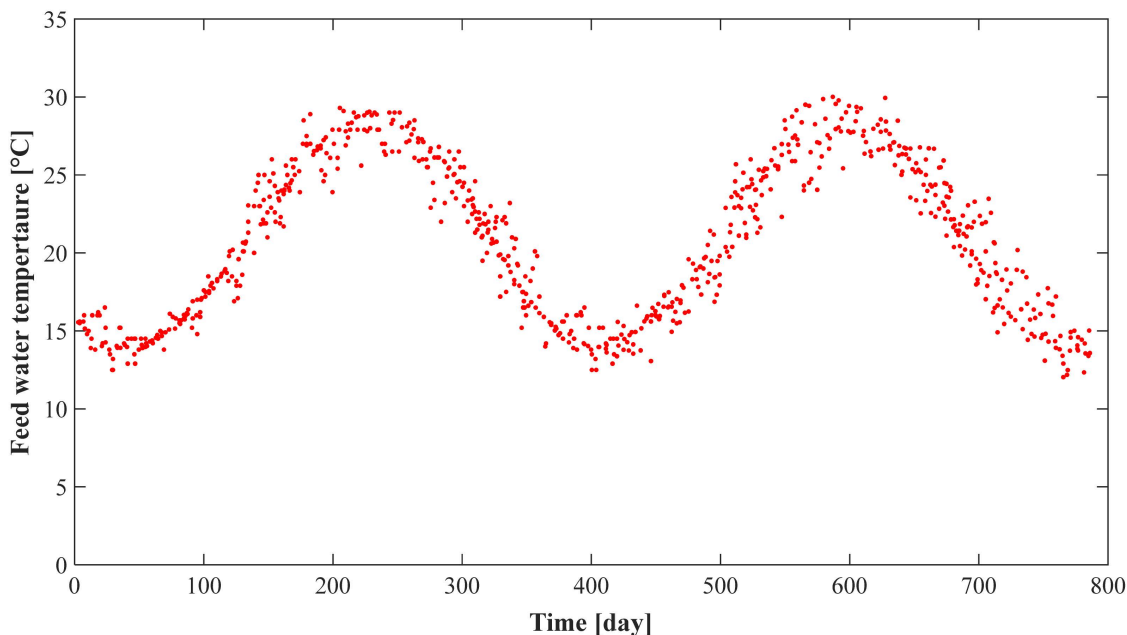


**Figure 3.** Variations in the feed water temperature during the monitoring period. Temperature variations are seasonal variations.

Feed water TDS variations with respect to operating time are displayed in Figure 4. As shown in the figure, feed water TDS remained quite stable with a less than 5.0% variation around the mean value (46 412 mg/L) over the monitoring period.

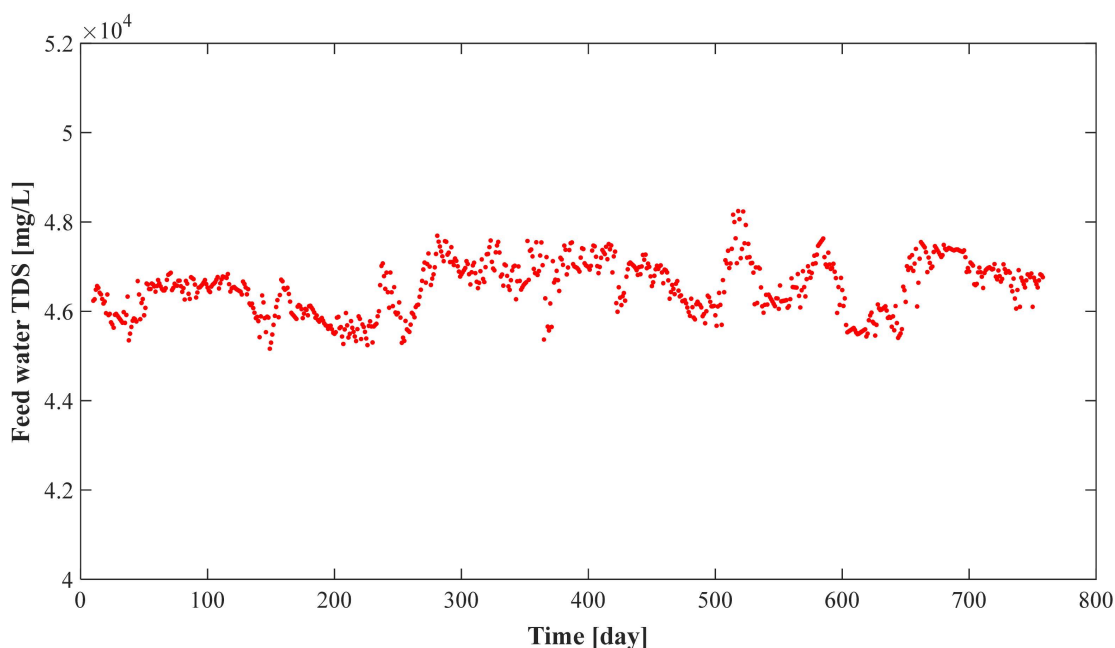


**Figure 4.** Variations in the feed water TDS during the monitoring period.

Feed water flow rate and pressure are displayed in Figures 5 and 6. The feed flow rate slightly varies around its average value (72,356 m<sup>3</sup>/day). This is expected since the RO facility was operated at constant flux. Feed pressure also remained stable with a less than 5.0% variation around the mean value (71.2 bar).

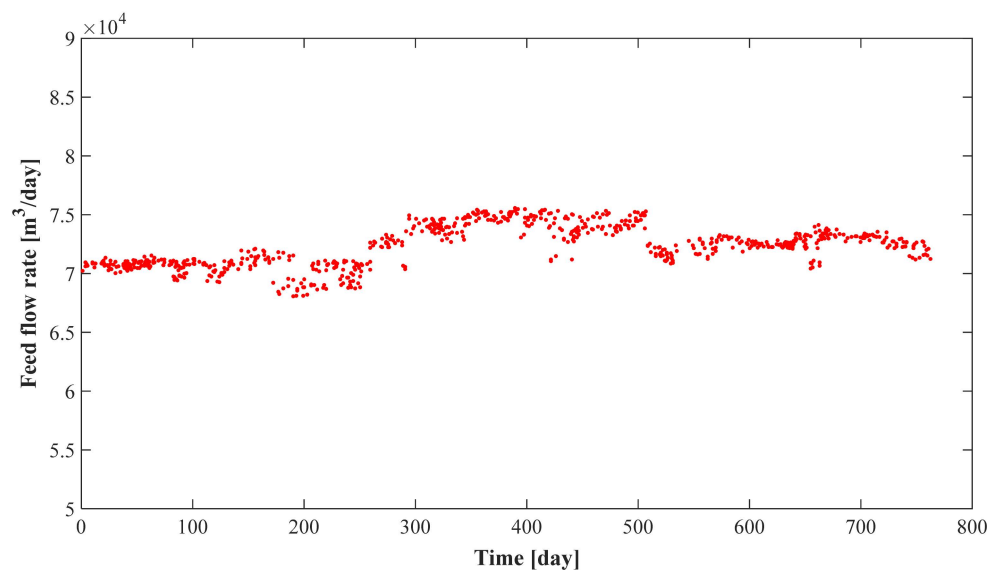


**Figure 5.** Variations in the feed flow rate during the monitoring period.

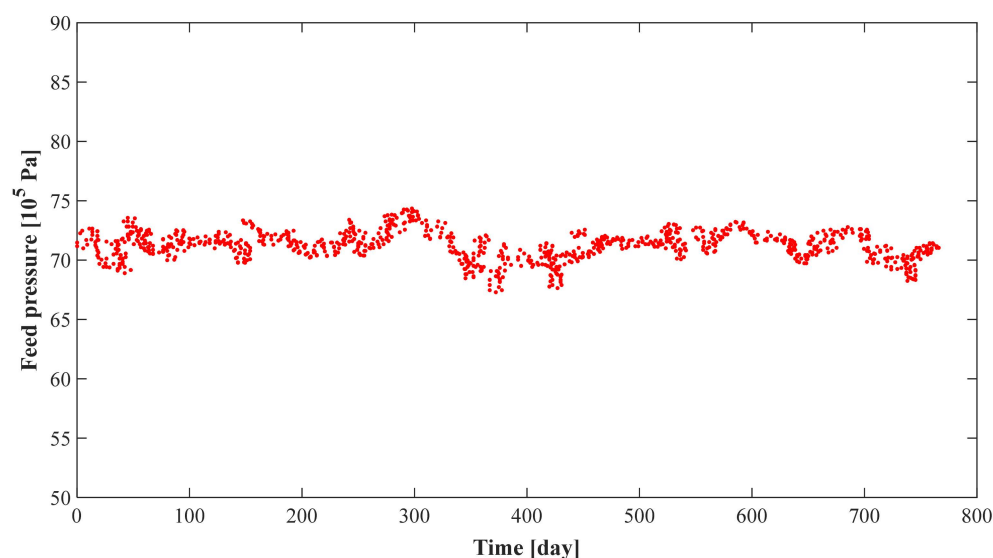


**Figure 6.** Variations in the feed water pressure during the monitoring period.

A larger variation is noticed when the permeate TDS is considered (Figure 7). Data showed that the permeate TDS greatly varied. This could be related to the variations in the feed water temperature. It is known that high temperatures increase membrane salt passage, which inevitably leads to augmented TDS for the permeate. Membrane fouling can also increase the permeate TDS concentration. This is because the foulants can act as a barrier to the passage of water molecules, but they allow salt ions to pass through more easily. As a result, salt rejection by the membrane decreases, and the permeate TDS concentration increases. This phenomenon is evidenced by the decrease in permeate TDS after each membrane cleaning (MC) event. A few weeks after membrane cleaning, membranes start to be progressively fouled, causing the permeate TDS to peak again. In Figure 7, the permeate TDS starts to increase progressively from a value approaching 56 mg/L (at 100 days) to reach a value of 92 mg/L (at 255 days). The membrane cleaning performed at 260 days caused the permeate TDS to progressively decrease before it increased again after 120 days.

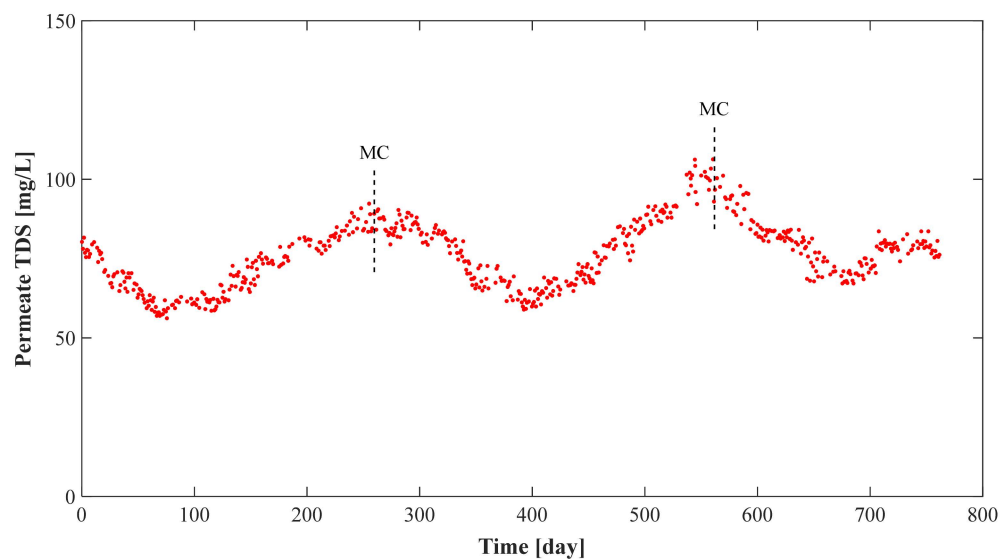


**Figure 7.** Evolution of the permeate TDS during the monitoring period. Membrane cleaning events are marked in the figure.

The evolution of the pressure drop with respect to operating time is displayed in Figure 8. Similar to the permeate TDS, the pressure drop shows variations that can be correlated with the membrane cleaning events. However, the variations in the pressure drop are less pronounced when compared with those in the permeate TDS. Physically, fouling reduces the membrane's permeability, which decreases the permeate flow rate and increases the pressure drop.

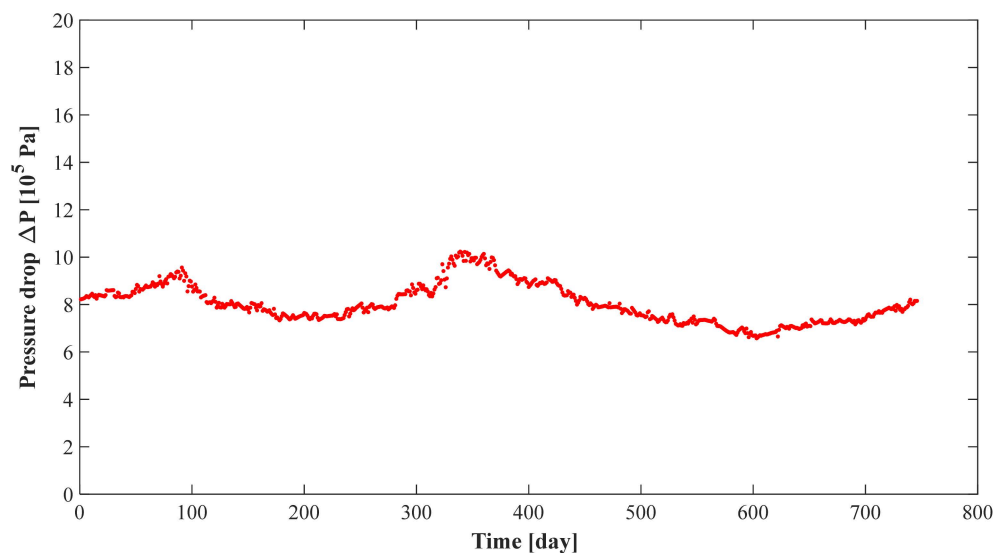


**Figure 8.** Evolution of the pressure drop during the monitoring period.

#### 4.3. PINN Training and Testing

The PINN approach described in Section 3 is employed to predict the performance of the studied SWRO desalination process. The experimental dataset including measurements undertaken for 760 operating days is employed to build a prediction model for the produced water quality and quantity. For all training cases,  $k$ -fold cross-validation is employed with  $k = 5$ . Following this validation method, the training set is split into  $k$  equal parts (called folds). In each training iteration,  $(k - 1)$  folds are used for training while the remaining fold is used as the test set. This procedure is repeated until all folds are used. After  $k$  iterations,

the model is validated on every fold, which is assumed to give more stable and trustworthy results since training and testing are performed on several different parts of the dataset.

For the evaluation of the created ML models, three metrics are employed: the determination coefficient ( $R^2$ ), the mean absolute error (MAE), and the root mean squared error (RMSE). Generally, lower values are the target for MAE and RMSE. For the determination coefficient, values close to one indicate better model performance. These performance criteria are expressed in Equations (12)–(14).

$$R^2 = 1 - \frac{\sum_{i=1}^N (y_{i,p} - y_{i,o})^2}{\sum_{i=1}^N (y_{i,o} - y_{o,m})^2} \quad (12)$$

$$MAE = \frac{1}{N} \sum_{i=1}^N |y_{i,p} - y_{i,o}| \quad (13)$$

$$RMSE = \sqrt{\frac{\sum_{i=1}^N (y_{i,p} - y_{i,o})^2}{N}} \quad (14)$$

where  $y_{i,p}$ ,  $y_{i,o}$ , and  $y_{o,m}$  are predicted, observed, and average observed values, and  $N$  is the total number of data points.

The best predictive model is exported as a Matlab<sup>®</sup> (version 2021a) function to be used to generate predicted responses for new input data.

## 5. Results and Discussion

Two operation parameters are chosen to showcase the effectiveness of the proposed PINN-based modeling methodology: the predicted values of the permeate TDS and the pressure drop. These predicted values are displayed with respect to the actual measured values in Figure 9. Figure 9a shows predicted and experimental values of the permeate TDS. The results indicate that the predicted values obtained using PINN exhibited a strong correlation, as evidenced by a determination coefficient of 0.96. In Figure 9b, the predicted values of the pressure drop are compared with the measured values at the SWRO plant. Again, the displayed results show a strong correlation between the measured and predicted values.

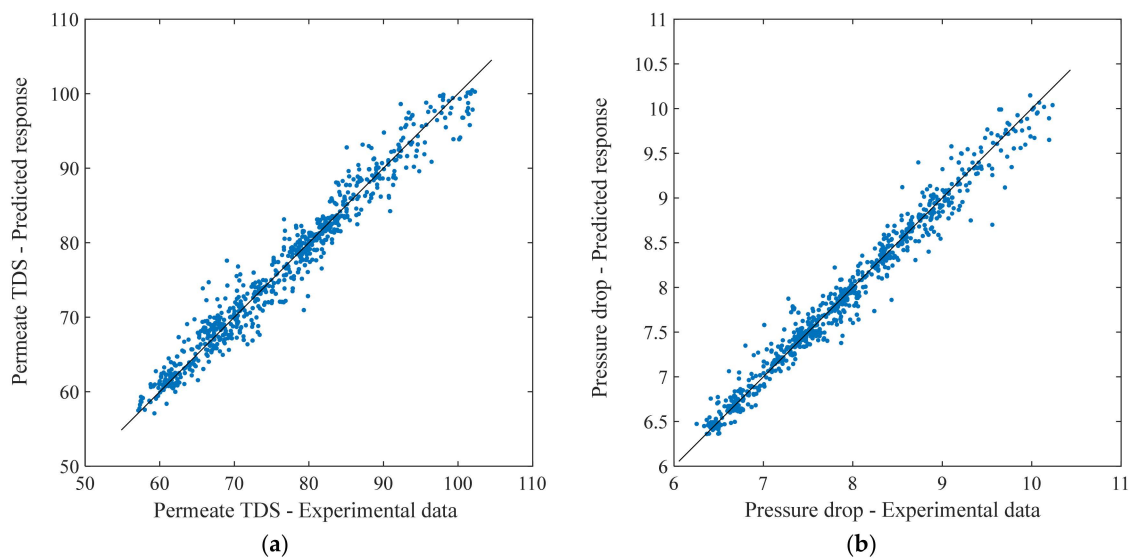


**Figure 9.** Comparing PINN model prediction with experimental operating data for (a) the permeate TDS and (b) the pressure drop.

The performances of the studied PINN in modeling the permeate TDS and the pressure drop in the studied RO plant were assessed and the results are presented in Table 2. It can be concluded from the performance results in Table 2 that the two PINN-based models have high prediction performance associated with strong generalization potential. These prediction models offer great opportunities to be used as the basis for performance optimization avoiding expensive and time-consuming experimental investigations as well as inaccuracies that could be associated with analytical formulations.

**Table 2.** Performances of the PINN models.

Output Parameter	Metrics		
	RMSE	R <sup>2</sup>	MAE
Permeate TDS	2.0773	0.96	1.5538
Pressure drop	0.1417	0.97	0.1009

The comparison between measured and predicted permeate TDS with respect to operating time is shown in Figure 10. The PINN model shows good consistency with the experimental results, which means that the PINN model can predict the permeate TDS accurately. The evolution of the pressure drop with respect to operating time is displayed in Figure 11. The trend is similar to that in Figure 10. The PINN model shows good consistency with the measured values. These results confirm that PINN-based models have high prediction performance associated with strong generalization potential.

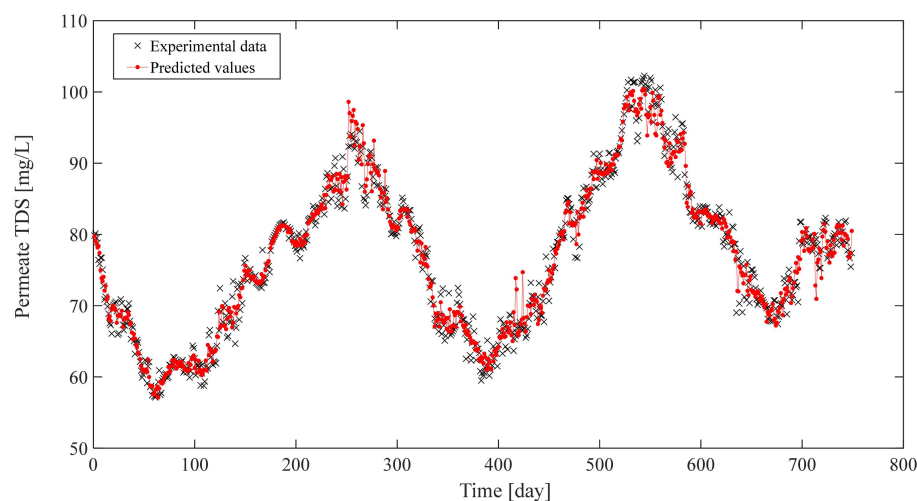


**Figure 10.** Comparing PINN model prediction with experimental operating data for the permeate TDS.

In order to showcase the prediction potential of the PINN-based models, hand-generated data for feed water temperature, feed water TDS, and feed flow rate are used as input for the prediction model. Feed water temperature values were generated according to the seasonal variation trend (Figure 3), whereas feed water TDS and feed water flow rate were randomly generated around their mean values using a fixed variation level of 5%. A fictitious membrane cleaning event was also simulated (day 820). Two hundred new records were hand-generated in this way and fed to the PINN models. A sample output is displayed in Figure 12, where the permeate TDS is predicted for the new data (from day 750 to day 949). Results show that the model can predict the evolution of the permeate TDS, which could help in scheduling operation maintenance tasks such as membrane cleaning. Using the developed model it is also possible to monitor the behavior of the RO process in real time. Monitoring the process behavior allows deviations from baseline operation to be

detected before they reach a critical level, thus preventing expensive maintenance measures. It is important to note that the proposed methodology could be a step toward achieving efficient and physically meaningful modeling for RO plants. Even if the presented results are firmly related to the specific RO desalination plant where the data were collected, it is important to note that the methodology itself is scalable and simply applicable in any other RO plant if enough operating data is available.

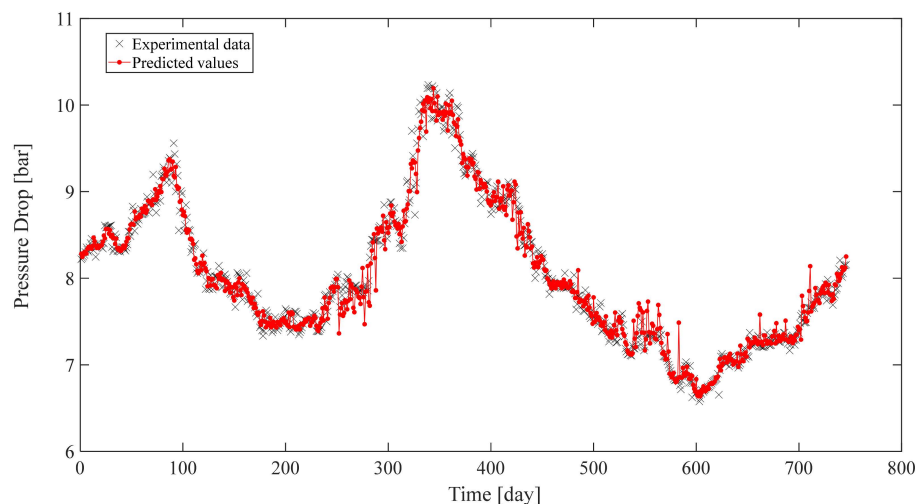


**Figure 11.** Comparing PINN model prediction with experimental operating data for pressure drop.

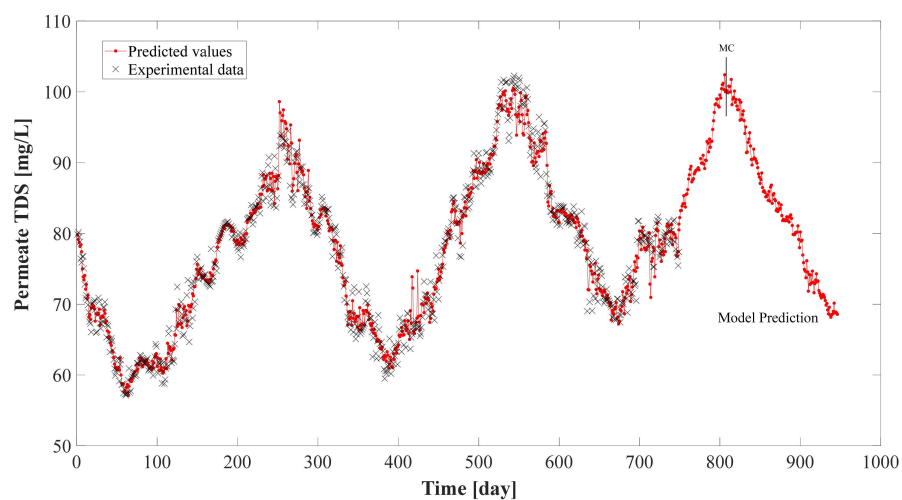


**Figure 12.** Predicted permeate TDS based on the PINN model.

## 6. Conclusions

In this paper, physics-informed neural network models are proposed to predict some operating parameters of a full-scale RO plant. The proposed models are trained to predict the effects of operating conditions on the permeate TDS and pressure drop. The tested PINN showed high performance with a determination coefficient of 0.96 for the permeate TDS model and 0.97 for the pressure drop model.

The preliminary results obtained in this study emphasize the potential of using PINNs for modeling the RO desalination process. Data-driven models can be employed at little to no cost, avoiding expensive and time-consuming experimental investigations. Furthermore, PINNs that incorporate physical information can provide interpretable and physically meaningful neural network models that are obviously more accurate and general than models that are created based on data only. This makes PINNs well-suited for modeling

complex processes such as RO. Furthermore, prediction models created using PINNs are also able to learn the process characteristics that affect its overall performance and can help RO plant operators adapt to changes in operating conditions.

Finally, the PINN modeling approach proposed here for some RO operating parameters can be adapted to be efficiently used for other process parameters such as recovery and specific energy consumption (SEC) in order to overcome the limitations related to experimentally extracting physical quantities and the inaccuracies generally associated with simple analytical models. Further research is needed to improve the prediction models created using PINNs and to use them for operation optimization and aiding decision-making. It is also important to tackle specific aspects such as the intermittency of RO plant operations. The authors believe that the described PINN-based methodology is promising and could be part of future endeavors.

**Author Contributions:** Methodology, N.B.H.A., S.H. and S.A.; Software, N.B.H.A.; Formal analysis, S.H. and N.B.H.A.; Resources, S.H.; Writing—original draft, S.H. and N.B.H.A.; Writing—review & editing, S.H. and S.A.; Visualization, S.A. All authors have read and agreed to the published version of the manuscript.

**Funding:** This research received no external funding.

**Data Availability Statement:** Data are contained within the article.

**Conflicts of Interest:** The authors declare no conflict of interest.

## Nomenclature

### Acronyms

Permeate flux	$J_w$
Membrane permeability coefficient	$A_w$
Permeate flow rate	$Q_p$
Total membrane area	$S_m$
Solute flux	$J_s$
Solute permeability coefficient	$B_s$
Solute concentration in the feed	$C_f$
Solute concentration in the permeate	$C_p$
Osmotic pressure of the membrane	$\pi_m$
Permeate osmotic pressure	$\pi_p$
Feed water pressure	$P_f$
Pressure drop at the feed side of the membrane	$\Delta P_{fb}$
Recovery rate	$R$
Feed water flow rate	$Q_f$
Total Dissolved Solids	$TDS$
Mean absolute error	$MAE$
Root mean squared error	$RMSE$
<b>Physics-Informed Neural Networks</b>	
Neural network with	$\mathcal{N}(x; \theta)$
Weights	$\theta$
Loss function	$\mathcal{L}_0$
Physics-informed term	$\mathcal{L}_{Phys}$

## References

- Engin, K.; Richard, C. *The United Nations World Water Development Report 2023: Partnerships and Cooperation for Water*; UN-ESCO: Paris, France, 2023.
- Baggio, G.; Qadir, M.; Smakhtin, V. Freshwater availability status across countries for human and ecosystem needs. *Sci. Total Environ.* **2021**, *792*, 148230. [[CrossRef](#)] [[PubMed](#)]

3. Ayaz, M.; Namazi, M.; Din, M.A.U.; Ershath, M.M.; Mansour, A.; Aggoune, E.-H.M. Sustainable seawater desalination: Current status, environmental implications and future expectations. *Desalination* **2022**, *540*, 116022. [\[CrossRef\]](#)
4. Curto, D.; Franzitta, V.; Guercio, A. A Review of the Water Desalination Technologies. *Appl. Sci.* **2021**, *11*, 670. [\[CrossRef\]](#)
5. Jeong, K.; Park, M.; Ki, S.J.; Kim, J.H. A systematic optimization of Internally Staged Design (ISD) for a full-scale reverse osmosis process. *J. Membr. Sci.* **2017**, *540*, 285–296. [\[CrossRef\]](#)
6. Qasim, M.; Badrelzaman, M.; Darwish, N.N.; Hilal, N. Reverse osmosis desalination: A state-of-the-art review. *Desalination* **2019**, *459*, 59–104. [\[CrossRef\]](#)
7. Jawad, J.; Hawari, A.H.; Zaidi, S.J. Artificial neural network modeling of wastewater treatment and desalination using membrane processes: A review. *Chem. Eng. J.* **2021**, *419*, 129540. [\[CrossRef\]](#)
8. Srivastava, A.; Nair, A.; Ram, S.; Agarwal, S.; Ali, J.; Singh, R.; Garg, M.C. Response surface methodology and artificial neural network modelling for the performance evaluation of pilot-scale hybrid nanofiltration (NF) & reverse osmosis (RO) membrane system for the treatment of brackish ground water. *J. Environ. Manag.* **2020**, *278*, 111497. [\[CrossRef\]](#)
9. Niu, C.; Li, X.; Dai, R.; Wang, Z. Artificial intelligence-incorporated membrane fouling prediction for membrane-based processes in the past 20 years: A critical review. *Water Res.* **2022**, *216*, 118299. [\[CrossRef\]](#)
10. Choi, Y.; Lee, Y.; Shin, K.; Park, Y.; Lee, S. Analysis of long-term performance of full-scale reverse osmosis desalination plant using artificial neural network and tree model. *Environ. Eng. Res.* **2019**, *25*, 763–770. [\[CrossRef\]](#)
11. Yang, Y.; Wang, C.; Wang, S.; Xiao, Y.; Ma, Q.; Tian, X.; Zhou, C.; Li, J. Performance prediction model for desalination plants using modified grey wolf optimizer based artificial neural network approach. *Desalination Water Treat.* **2024**, *319*, 100411. [\[CrossRef\]](#)
12. Bonny, T.; Kashkash, M.; Ahmed, F. An efficient deep reinforcement machine learning-based control reverse osmosis system for water desalination. *Desalination* **2022**, *522*, 115443. [\[CrossRef\]](#)
13. Mohammed, A.; Alshraideh, H.; Alsuwaidi, F. A holistic framework for improving the prediction of reverse osmosis membrane performance using machine learning. *Desalination* **2023**, *574*, 117253. [\[CrossRef\]](#)
14. Mahadeva, R.; Kumar, M.; Gupta, V.; Manik, G.; Gupta, V.; Alawatugoda, J.; Manik, H.; Patole, S.P.; Gupta, V. Water desalination using PSO-ANN techniques: A critical review. *Digit. Chem. Eng.* **2023**, *9*, 100128. [\[CrossRef\]](#)
15. Mahadeva, R.; Kumar, M.; Gupta, V.; Manik, G.; Patole, S.P. Modified Whale Optimization Algorithm based ANN: A novel predictive model for RO desalination plant. *Sci. Rep.* **2023**, *13*, 2901. [\[CrossRef\]](#)
16. Karimanzira, D.; Rauschenbach, T. Performance Prediction of a Reverse Osmosis Desalination System Using Machine Learning. *J. Geosci. Environ. Prot.* **2021**, *9*, 46–61. [\[CrossRef\]](#)
17. Nazari, M.A.; Salem, M.; Mahariq, I.; Younes, K.; Maqableh, B.B. Utilization of Data-Driven Methods in Solar Desalination Systems: A Comprehensive Review. *Front. Energy Res.* **2021**, *9*, 742615. [\[CrossRef\]](#)
18. Cuomo, S.; Di Cola, V.S.; Giampaolo, F.; Rozza, G.; Raissi, M.; Piccialli, F. Scientific Machine Learning Through Physics-Informed Neural Networks: Where we are and What's Next. *J. Sci. Comput.* **2022**, *92*, 88. [\[CrossRef\]](#)
19. Kim, D.; Lee, J. A Review of Physics Informed Neural Networks for Multiscale Analysis and Inverse Problems. *Multiscale Sci. Eng.* **2024**, *6*, 1–11. [\[CrossRef\]](#)
20. Raissi, M.; Perdikaris, P.; Karniadakis, G.E. Physics-informed neural networks: A deep learning framework for solving forward and inverse problems involving nonlinear partial differential equations. *J. Comput. Phys.* **2019**, *378*, 686–707. [\[CrossRef\]](#)
21. Habib, A.; AL Hourri, A.; Junaid, M.T.; Barakat, S. A systematic and bibliometric review on physics-based neural networks applications as a solution for structural engineering partial differential equations. *Structures* **2024**, *69*, 107361. [\[CrossRef\]](#)
22. Karniadakis, G.E.; Kevrekidis, I.G.; Lu, L.; Perdikaris, P.; Wang, S.; Yang, L. Physics-informed machine learning. *Nat. Rev. Phys.* **2021**, *3*, 422–440. [\[CrossRef\]](#)
23. Al-Obaidi, M.; Kara-Zaitri, C.; Mujtaba, I. Scope and limitations of the irreversible thermodynamics and the solution diffusion models for the separation of binary and multi-component systems in reverse osmosis process. *Comput. Chem. Eng.* **2017**, *100*, 48–79. [\[CrossRef\]](#)
24. Al-Obaidi, M.; Alsarayreh, A.; Al-Hroub, A.; Alsadaie, S.; Mujtaba, I. Performance analysis of a medium-sized industrial reverse osmosis brackish water desalination plant. *Desalination* **2018**, *443*, 272–284. [\[CrossRef\]](#)
25. Ruiz-García, A.; Nuez-Pestana, I.d.l. A computational tool for designing BWRO systems with spiral wound modules. *Desalination* **2018**, *426*, 69–77. [\[CrossRef\]](#)
26. Sayyad, S.; Kamthe, N.; Sarvade, S. Design and simulation of reverse osmosis process in a hybrid forward osmosis-reverse osmosis system. *Chem. Eng. Res. Des.* **2022**, *183*, 210–220. [\[CrossRef\]](#)
27. Saeed, A.; Alhawaj, M. Mathematical modeling of reverse osmosis system design and performance. *Water Pract. Technol.* **2024**, *19*, 2681–2692. [\[CrossRef\]](#)
28. Ruiz-García, A.; Nuez, I. Long-term performance decline in a brackish water reverse osmosis desalination plant. Predictive model for the water permeability coefficient. *Desalination* **2016**, *397*, 101–107. [\[CrossRef\]](#)

29. AlSawaftah, N.; Abuwatfa, W.; Darwish, N.; Hussein, G. A Comprehensive Review on Membrane Fouling: Mathematical Modelling, Prediction, Diagnosis, and Mitigation. *Water* **2021**, *13*, 1327. [[CrossRef](#)]
30. Jiang, A.; Ding, Q.; Wang, J.; Jiangzhou, S.; Cheng, W.; Xing, C. Mathematical Modeling and Simulation of SWRO Process Based on Simultaneous Method. *J. Appl. Math.* **2014**, *2014*, 908569. [[CrossRef](#)]

**Disclaimer/Publisher's Note:** The statements, opinions and data contained in all publications are solely those of the individual author(s) and contributor(s) and not of MDPI and/or the editor(s). MDPI and/or the editor(s) disclaim responsibility for any injury to people or property resulting from any ideas, methods, instructions or products referred to in the content.